

Electroweak Cross-sections and Widths

A. Robson (on behalf of the CDF and D0 Collaborations)
Glasgow University, Glasgow G12 8QQ, UK

The status of W and Z cross-section and width measurements from the CDF and D0 experiments is reviewed. Recent results that are discussed: the cross-section for Z production times the branching ratio to tau pairs, the rapidity and transverse momentum distributions of Z production in the electron channel, and the direct measurements of the W width and the Z invisible width; the latter from an analysis of events with large missing transverse energy and one or more energetic jets.

1. W AND Z PHYSICS AT THE TEVATRON

Already early in Run 2 of the Tevatron, using less than 100 pb^{-1} of data, total inclusive W and Z cross-section measurements were essentially systematically limited [1]. From the theoretical side, W and Z cross-sections are well-known, fully differentially to NNLO. From an experimental point of view, the Tevatron W and Z boson datasets provide a pure sample of high- p_T electrons and muons. Now with more than thirty times the statistics of those early measurements, the W and Z datasets provide a powerful tool for lepton reconstruction, identification and trigger measurements. But at a fundamental level, total inclusive W and Z cross-section measurements are benchmarks for all high- p_T physics analyses.

A tower of physics measurements is built on the selection of W and Z events. W and Z plus photon measurements and heavy diboson WW, WZ and ZZ measurements probe triple gauge couplings; and the precision of top-quark cross-sections continues to improve. Each of these measurements needs to demonstrate consistent determinations of inclusive W and Z cross-sections as a test of the implementation of selections, efficiencies, good run lists and luminosity computations. Observations of the rarer processes can be seen as stations on the way to a heavy Higgs boson, decaying to a pair of W bosons [2].

However dedicated measurements on single W and Z events also continue. Their focus now is on the more challenging tau decay modes, and on using the large datasets to make differential cross-section measurements in order to look for discrepancies with higher-order calculations and to test the edges of phase space, and to make high-precision measurements of Standard Model parameters such as masses and widths.

2. Z $\rightarrow \tau\tau$

Tau leptons are more complex objects to reconstruct than electrons or muons, and measurement techniques continue to improve. At D0, τ identification starts from calorimeter clusters, reconstructed in a cone of $\Delta R < 0.5$, that have their energy concentrated in an inner cone of $\Delta R < 0.3$. The tracks within the inner cone are required to be consistent with a tau, such that $m_{\text{tracks}} < 1.8 \text{ GeV}$. The electromagnetic clusters are considered in terms of sub-clusters, reconstructed from a seed in the most finely segmented ‘shower-maximum’ layer of the calorimeter.

Tau candidates are assigned to one of three categories, according to the number of tracks and subclusters. The categories correspond broadly to one-prong, one-prong plus neutral, and three-prong tau decays.

To improve the selection, neural nets are trained for each category on variables that characterise the isolation, shower shape, and correlations between the tracks and clusters. This results in excellent background suppression.

Furthermore, recent improvements in the τ energy corrections have significantly reduced uncertainties.

D0 selects $Z \rightarrow \tau_\mu \tau_h$ from an inclusive muon trigger. Both the muon and tau have $p_T > 15 \text{ GeV}$, and in addition there is a minimum requirement on the scalar sum- p_T of the tau tracks. The leptons have opposite charge.

A data-driven estimate of the QCD background, which is mostly $b\bar{b}$, is obtained from same-charge events, and corrected for the expected rate of same-charge events from a QCD-enhanced dataset. Electroweak backgrounds are

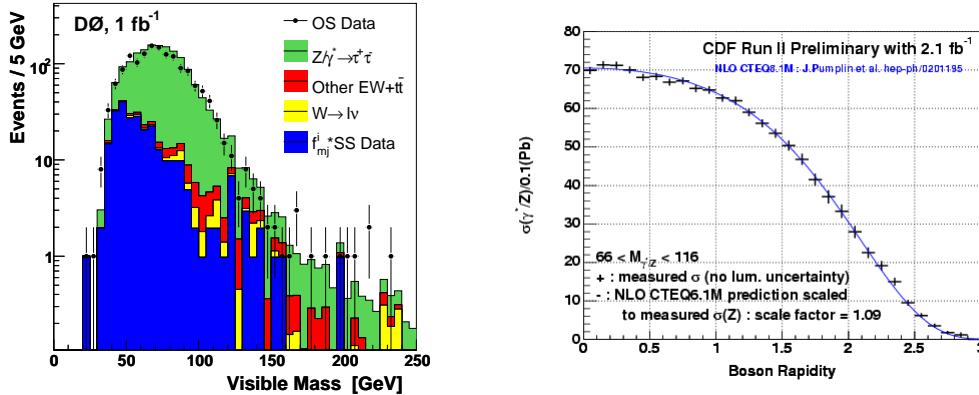


Figure 1: (left) The ‘visible mass’, $m_{\text{vis}} = \sqrt{(P_{\mu} + P_{\tau} + H_T)^2}$, for $Z \rightarrow \tau_{\mu} \tau_{\text{h}}$ candidates. (right) The Z rapidity distribution.

obtained from simulation, and the W plus jets background is corrected for the component already accounted for in the same-charge events. The background uncertainties are much reduced compared to previous D0 measurements.

The resulting selection is shown in Figure 1. 1511 events are observed, of which around 20% are background. A cross-section is extracted: $\sigma(p\bar{p} \rightarrow Z) \cdot Br(Z \rightarrow \tau\tau) = 240 \pm 8(\text{stat}) \pm 12(\text{sys}) \pm 15(\text{lumi}) \text{ pb}$ [3].

3. Z RAPIDITY

In Z boson production, the rapidity $y = \frac{1}{2} \ln \frac{E+p_z}{E-p_z}$ is closely related to the momentum fractions x of the interacting partons: at leading order the relation is $x_{1,2} = \frac{m_Z}{\sqrt{s}} e^{\pm y}$. Measuring the Z boson rapidity is therefore a direct probe of the PDFs of the interacting partons.

Furthermore, at CDF, Z bosons can be reconstructed over the entire kinematic range in the electron channel, using the forward calorimeters. This gives access to events at very low x , where PDFs are relatively uncertain.

Events are selected in three topologies, according to whether the electrons are reconstructed in the central or forward parts of the detector.

Backgrounds are estimated in a data-driven way, by forming signal and background templates of the electron isolation distribution, and extrapolating the non-isolated tail into the low isolation signal region.

The acceptance as a function of rapidity is taken from simulation, and the rapidity dependences of the electron identification efficiencies are determined.

The measured rapidity distribution is shown in Figure 1. Whereas previous versions of this measurement have been entirely statistically dominated, the current large dataset results in systematic uncertainties comparable with the statistical uncertainties in some regions of rapidity. Comparison is made with an NNLO calculation and NNLO PDFs, and with an NLO calculation and several NLO PDFs. Although at present the measurement does not clearly favour one set over another, with even more statistics there could be some scope for constraining PDFs.

4. Z TRANSVERSE MOMENTUM

Measuring the p_T of the Z tests QCD predictions for initial state gluon radiation. Whereas the high end of the p_T spectrum (above $\sim 30 \text{ GeV}/c$) is dominated by single hard emissions and perturbative QCD is reliable, the low end of the spectrum is dominated by multiple soft gluon radiation, which must be calculated by resummation or modelled by a non-perturbative parton shower monte carlo. The RESBOS event generator implements NLO QCD and the CSS resummation formalism, using the BNLY form-factor and parameters determined by global fits to DIS and fixed-target data. This is a particularly interesting time to be probing this model, as recent global fits have

suggested the presence of an extra contribution to the form-factor at small x . This would imply a broadening of the $Z p_T$ at high rapidities ($|y_Z| > 2$) at the Tevatron, and a significant effect on centrally-produced W and Z bosons at the LHC. D0 has looked for evidence of this effect [4].

In 1 fb^{-1} , around 64000 Z events are reconstructed in the electron channel, of which around 5000 have $|y_Z| > 2$. Backgrounds are estimated from templates fitted to the mass distribution m_{ee} . A regularized unfolding technique is used to reconstruct the underlying p_T distribution. The low end of the Z p_T distribution for all rapidities is compared to the RESBOS prediction, and found to be in good agreement. The Z p_T for events that have $|y_Z| > 2$ is compared to RESBOS predictions both with and without the extra small- x form-factor, as shown in Figure 2. Without the small- x form-factor the fit is found to be $\chi^2/\text{dof}=11.1/11$, whereas with the extra term the fit is $\chi^2/\text{dof}=31.9/11$. This measurement therefore disfavours the small- x broadening.

It is interesting to note that when the complete Z p_T spectrum is examined, a NNLO calculation reproduces the shape well, but requires rescaling by 25% to match the normalisation.

5. W WIDTH

The width of the W boson is predicted very precisely in the Standard Model, and so its accurate measurement is a powerful check of the consistency of the Standard Model. CDF has measured Γ_W using 350 pb^{-1} of data [5].

Experimentally, transverse quantities are accessible at the Tevatron; for example the transverse mass $m_T = \sqrt{2p_T^\ell p_T^\nu (1 - \cos \phi_{\ell\nu})}$. Events can have $m_T > m_W$ either as a result of the intrinsic W width, or as a result of detector smearing. The Gaussian effects of detector smearing are found to fall faster than the intrinsic Breit-Wigner lineshape, so the procedure for measuring the width is to use the region $m_T < 90 \text{ GeV}/c^2$ for normalisation, and to fit templates to the high m_T region.

Events to construct the templates are taken from a leading-order monte carlo, matched with RESBOS for QCD initial state radiation and with a calculation from Berends and Kleiss for QED final state radiation. A fast simulation models electron conversion and showering, muon energy loss, and includes a parametric model of the energy in the detectors not associated with the high- p_T electron or muon (the ‘recoil energy’), which originates from QCD, the underlying event and bremsstrahlung. The final uncertainty on Γ_W from the recoil modeling is $\Delta\Gamma = 54 \text{ MeV}$ and $\Delta\Gamma = 49 \text{ MeV}$ in the electron and muon channels respectively. The modeling of the tracking scale and resolution and the calorimeter energy scale and resolution are checked on $Z \rightarrow \mu\mu$ and $Z \rightarrow ee$ events respectively; and also on the J/ψ . Uncertainties from the tracking scale and resolution are $\Delta\Gamma = 17; 26 \text{ MeV}$ ($e;\mu$) and from the calorimeter scale and resolution $\Delta\Gamma = 21; 31 \text{ MeV}$ ($e;\mu$). Backgrounds are dominated by QCD multijet events in the electron channel and by $Z \rightarrow \mu\mu$ and decays in flight in the muon channel ($\Delta\Gamma = 32; 33 \text{ MeV}$ ($e;\mu$)).

The fit in the muon channel is shown in Figure 2. The fits are excellent and the W width is found to be:

$$\Gamma_W = 2032 \pm 73(\text{stat} + \text{sys}) \text{ MeV}, \quad (1)$$

which is the world’s most precise single direct measurement. It is consistent with the Standard Model prediction ($\Gamma_W = 2093 \pm 2 \text{ MeV}$) [6] and with CDF’s earlier indirect measurement ($\Gamma_W^{\text{indirect}} = 2092 \pm 42 \text{ MeV}$) [1].

6. Z INVISIBLE WIDTH

The invisible width of the Z is measured very precisely indirectly from LEP: $\Gamma_Z(\text{invis}) = 500.8 \pm 2.6 \text{ MeV}$. However the LEP direct measurement, using single photon events, is much less precise: $\Gamma_Z(\text{invis}) = 503 \pm 16 \text{ MeV}$. An analogous measurement from CDF in 1 fb^{-1} [7], using events with a single jet and large missing E_T , is completely uncorrelated.

Single-jet events are selected from a missing E_T trigger. Independently, $\sigma(Z + 1 \text{ jet}) \cdot Br(Z \rightarrow \ell\ell)$ is measured from high- p_T lepton triggers. The ratio of invisible and visible widths can be written as the ratio of cross-sections:

$$\frac{\Gamma_Z^{\text{invis}}}{\Gamma_Z^{\ell\ell}} = \frac{\sigma(Z + 1 \text{ jet}) \cdot Br(Z \rightarrow \text{invis})}{\sigma(Z + 1 \text{ jet}) \cdot Br(Z \rightarrow \ell\ell)} = \frac{N_{\text{obs}} - N_{\text{bck}}}{\kappa \cdot \sigma(Z + 1 \text{ jet}) \cdot Br(Z \rightarrow \ell\ell) \cdot \mathcal{L}}, \quad (2)$$

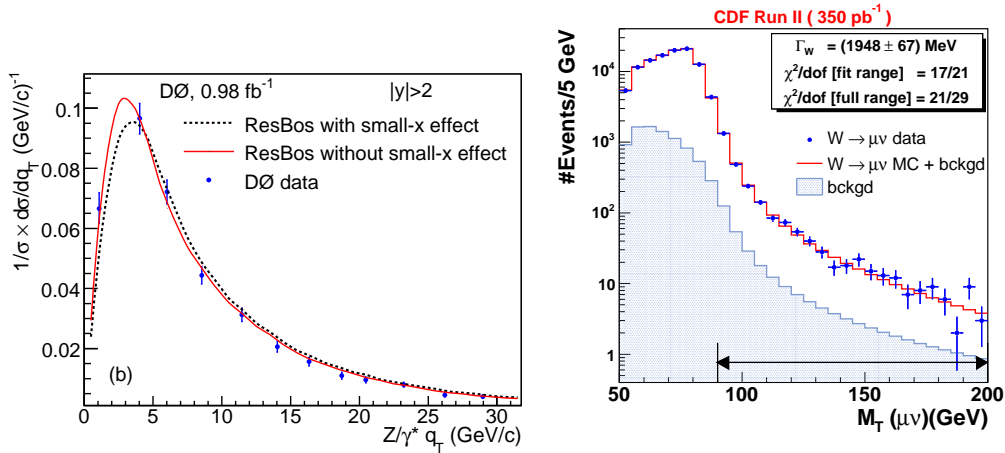


Figure 2: (left) The $Z p_T$ distribution for high-rapidity events. (right) The transverse mass fit in the muon channel.

where κ is a correction to take into account the different acceptance of the '+1 jet' selection in $Z \rightarrow \nu\nu$ events compared to $Z \rightarrow \ell\ell$ events.

The visible lepton cross-section is measured to be $\sigma(Z + 1 \text{ jet}) \cdot Br(Z \rightarrow \ell\ell) = 0.555 \pm 0.024 \text{ pb}$. This leads to an extracted value $\Gamma_Z^{\text{inv}} = 466 \pm 42 \text{ MeV}$, where the electroweak backgrounds, QCD backgrounds and visible lepton cross-section make approximately equal contributions to the uncertainty. This can also be interpreted as a measurement of the number of neutrino species, $N_\nu = 2.79 \pm 0.25$.

With more data this measurement could become competitive with those from the LEP experiments.

7. CONCLUSIONS

W and Z cross-section measurements underpin the Tevatron high- p_T physics programme. Dedicated measurements continue, harnessing the high statistics datasets: improving tau identification; testing higher-order calculations and PDFs and probing QCD; and making precision measurements of Standard Model parameters.

Acknowledgments

The author thanks the UK Science and Technology Facilities Council for financial support.

References

- [1] D. Acosta et al., Phys. Rev. Lett. **94** (2005) 091803; A. Aaltonen et al., J. Phys. G **34** (2007) 2457
- [2] A. Aaltonen et al., arXiv:0809.3930, submitted to Phys. Rev. L
- [3] V. Abazov et al., arXiv:0808.1306, submitted to Phys. Lett. B
- [4] V. Abazov et al., Phys. Rev. Lett. **100** (2008) 102002
- [5] A. Aaltonen et al., Phys. Rev. Lett. **100** (2008) 071801
- [6] P. Renton, arXiv:0804.4779
- [7] <http://www-cdf.fnal.gov/physics/ewk/2007/ZnumuWidth/>